

Galactic Radio Explorer: an all-sky monitor for bright radio bursts

LIAM CONNOR,¹ KIRAN A. SHILA,¹ SHRINIVAS R. KULKARNI,¹ JONAS FLYGARE,² GREGG HALLINAN,^{1,3} DONGZI LI,¹
WENBIN LU,¹ VIKRAM RAVI,¹ AND SANDER WEINREB¹

¹*Cahill Center for Astronomy and Astrophysics, MC 249-17, California Institute of Technology, Pasadena CA 91125, USA*

²*Onsala Space Observatory, Department of Space, Earth and Environment, Chalmers University of Technology
SE-41296 Gothenburg, Sweden*

³*Owens Valley Radio Observatory, MC 249-17, California Institute of Technology, Pasadena CA 91125, USA*

(Received November 24, 2021; Revised November 24, 2021; Accepted)

Submitted to Publications of the Astronomical Society of the Pacific

ABSTRACT

We present the Galactic Radio Explorer (GR_EX), an all-sky monitor to probe the brightest bursts in the radio sky. Building on the success of STARE2, we will search for fast radio bursts (FRBs) emitted from Galactic magnetars as well as bursts from nearby galaxies. GR_EX will search down to \sim ten microseconds time resolution, allowing us to find new super giant radio pulses from Milky Way pulsars and study their broadband emission. The proposed instrument will employ ultra-wide band (0.7–2 GHz) feeds coupled to a high performance (receiver temperature < 10 K) low noise amplifier (LNA) originally developed for the DSA-110 and DSA-2000 projects. In GR_EX Phase I (GR_EX-I), unit systems will be deployed at Owens Valley Radio Observatory (OVRO) and Big Smoky Valley, Nevada. Phase II will expand the array, placing feeds in India, Australia, and elsewhere in order to build up to continuous coverage of nearly 4π steradians and to increase our exposure to the Galactic plane. We model the local magnetar population to forecast for GR_EX, finding the improved sensitivity and increased exposure to the Galactic plane could lead to dozens of FRB-like bursts per year.

Keywords: fast radio bursts, pulsars, instrumentation

1. INTRODUCTION

The advent of wide-field, broad band radio surveys combined with our ability to search data at high time resolution has led to a number of novel discoveries. The fast radio burst (FRB) phenomenon in particular has radically changed the radio astronomy landscape (Cordes & Chatterjee 2019; Petroff et al. 2019). In response, many FRB surveys have been built or proposed.

The detection of a Galactic FRB from SGR 1935+2154 by both STARE2 and the Canadian Hydrogen Intensity Mapping Experiment (CHIME/FRB) was the most significant step to date in connecting extragalactic FRBs to a known phenomenon (The CHIME/FRB Collaboration et al. 2020; Bochenek et al. 2020b). The value of having such objects nearby is difficult to overstate, and detecting more ultra-bright bursts is essential to understanding the connection between magnetars and FRBs.

We propose the Galactic Radio Explorer (GR_EX, rhymes with “T-Rex”) as a complement to deeper, high-spatial resolution surveys. This is similar to how X-ray all-sky monitors and more sensitive instruments work symbiotically; GR_EX will detect rare ultra-bright Galactic bursts that cannot be discovered without nearly continuous all-sky monitoring. We are therefore building on the STARE2 design (Bochenek et al. 2020a), but with greater sensitivity, a five-times larger bandwidth, and clusters of antennas dispersed around the world. The GR_EX design is meant to maximize the detection rate of \sim MJy bursts per unit cost.

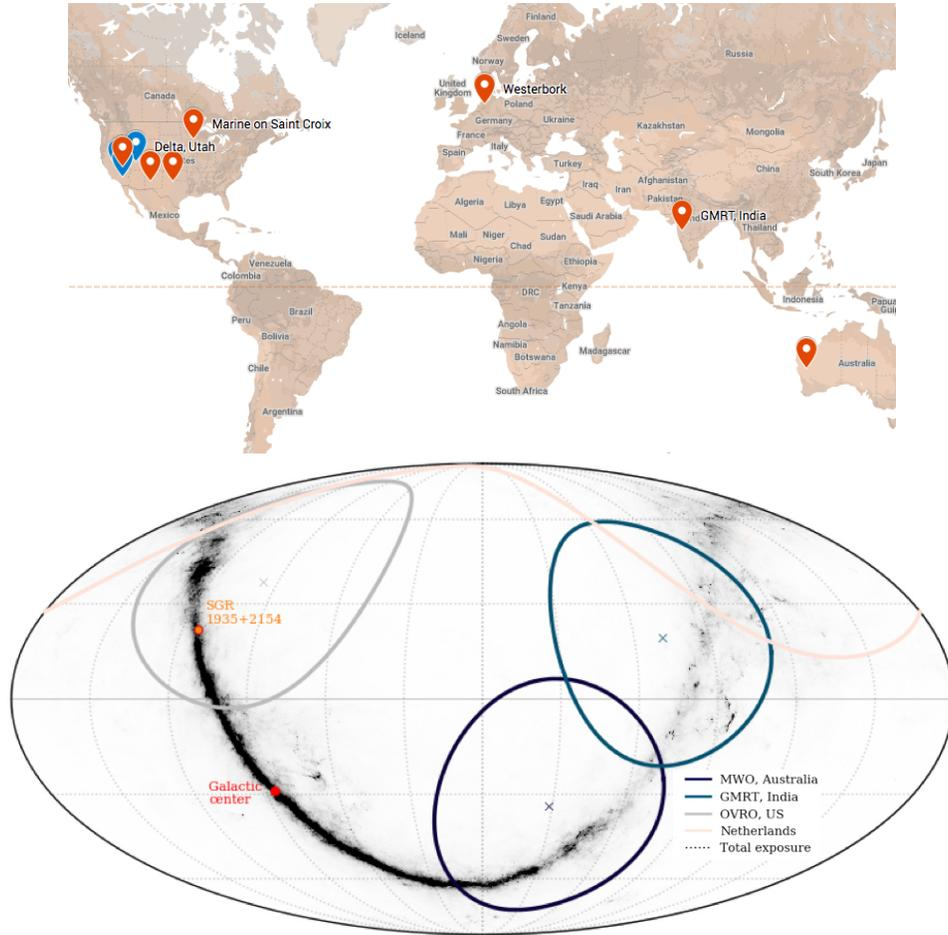


Figure 1. The layout of antenna clusters for GReX-I (blue) and GReX-II (red) is shown in the top figure. The bottom figure shows the instantaneous primary beam coverage of GReX clusters around the world, plotted over the Planck 857 GHz map (as a proxy for molecular gas and thus star-formation and Galactic magnetars). The first Galactic FRB (SGR 1935+2154) is marked in orange color. A hypothetical configuration of GReX-II, with three stations in India (marked “GMRT”), Australia, and the Netherlands each, would nicely cover the inner Galaxy (where bulk of the magnetars are located). It would also increase the coverage of the Northern sky.

FRBs have been detected over the frequency range 0.1 GHz to 8 GHz, though not simultaneously (Gajjar et al. 2018; Pastor-Marazuela et al. 2020; Pleunis et al. 2020). The angular distribution is approximately isotropic and the daily all-sky rate is $\sim 10^3$ with fluence above a few Jy ms (Petroff et al. 2019). The typical observed pulse widths are a few milliseconds, set by the \sim ms back-ends of most blind surveys; some FRBs are known to be tens to hundreds of microseconds in duration. A subset of 22 FRBs is known to repeat¹(Fonseca et al. 2020; CHIME/FRB Collaboration et al. 2019), and two of those repeaters appear to do so periodically on weeks to months timescales (Chime/Frb Collaboration et al. 2020; Rajwade et al. 2020). It is still unclear if repeating FRBs and those that have not been seen to repeat form two physically distinct classes, though there is evidence that their pulse morphology (Pleunis & Chime/Frb Collaboration 2021) and widths have different statistical distributions (Fonseca et al. 2020; Connor et al. 2020). Whether all FRBs are repeaters but with a large variation in time between bursts, or if there is a population of genuine once-off FRBs, remains one of the main outstanding questions in the field.

The events leading up to and during April 28, 2020 resulted in a dramatic link between magnetars and FRBs. On 27 April 2020, the Swift Burst Alert Telescope reported multiple bursts from the soft γ -ray repeater (SGR) 1935+2154, signaling that the magnetar had entered a phase of heightened activity. The next day the CHIME/FRB

¹ <https://www.chime-frb.ca/repeaters>

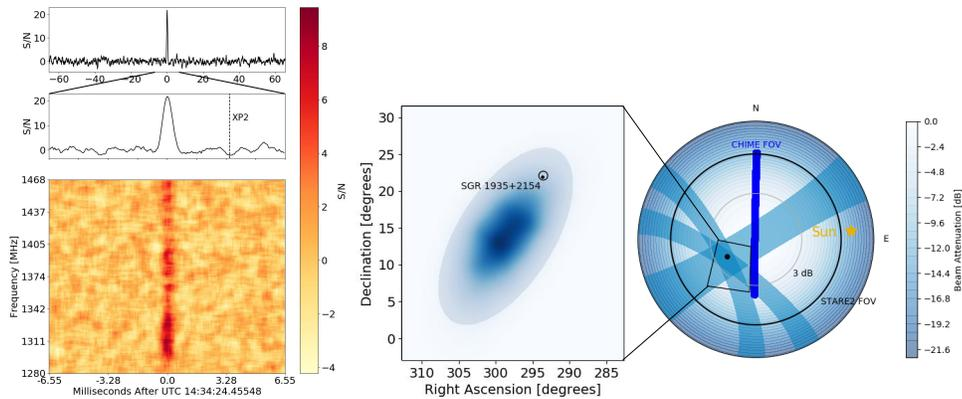


Figure 2. The dynamic spectrum of FRB 200428 from STARE2 (left), along with the combined localization region from its and CHIME/FRB’s detection (right). The STARE2 burst is centered on the X-ray emission.

collaboration reported a dispersed burst with \mathcal{F} of few kJy ms (0.4–0.8 GHz) in a side-lobe announced via ATel (Scholz & Chime/Frb Collaboration 2020), but this fluence value was later revised by a factor of 10^2 (The CHIME/FRB Collaboration et al. 2020). The daily inspection of recorded STARE2 triggers was then expedited, and ST 200428A was found at approximately at the same time and dispersion measure (DM) as the CHIME/FRB event. However, ST 200428A had a fluence that was a one thousand times greater than that reported by CHIME/FRB (Figure 2). Because this event was found in the complex sidelobes of CHIME, its fluence was simpler to measure in the STARE2 data. On 30 April 2020, the Five hundred metre Aperture Spherical Telescope (FAST) reported a weak (0.06 Jy ms) radio pulse and localized to SGR 1935+2154, with a DM consistent with the CHIME/FRB and STARE2 events.

Shortly thereafter, a constellation of space-borne instruments reported a one-second-long X-ray (1–250 keV) burst from the direction of SGR 1935+2154 that occurred at precisely the same time as the CHIME/FRB bursts and ST 200428A. This partnership between radio facilities (The CHIME/FRB Collaboration et al. 2020; Bochenek et al. 2020b; Zhang et al. 2020) is summarized graphically in Figure 2. Following the mega Jansky burst of 28 April, SGR 1935+2154 emitted intermittently bursts with fluence of 100 Jy ms (Kirsten et al. 2020) and has now finally become an intermittent pulsar at the X-ray period of 3.25s and fluence of 40 mJy ms (Zhu et al. 2020). Clearly, magnetars are capable of emitting mega Jansky bursts but not all magnetar X-ray flares are accompanied by intense radio bursts. We need more observations of this phenomenon to understand the currently murky X-ray-radio connection.

In this paper we first discuss the science that can be done with a global network of antennas searching the sky continuously at tens of microseconds. We then describe the novel hardware and digital back-end that have been developed for DSA-110 and DSA-2000, which will be modified for GREx. This includes an ultra-wide band feed, extremely low-noise amplifiers (LNAs), and a sub-band single pulse search strategy. In Sect. 4, we model the Galactic pulsar and magnetar distribution in order the forecast FRB and giant radio pulse science that will emerge from GREx.

2. SCIENCE GOALS

X-ray astronomy has shallow but very wide-field “all-sky monitors” or ASMs (e.g., Rossi X-ray Timing Explorer; MAXI) and also highly sensitive instruments (e.g., Rossi Proportional Counting Array; Chandra X-ray Observatory). The ASMs have historically played a major role in identifying rare but bright events that are missed by narrower field instruments. In the same way, as demonstrated by STARE2, radio astronomy would benefit from having a powerful radio ASM. GREx will fill this role.

Now let us examine the science drivers for GREx in some detail. Connor (2019) has analyzed the performance of FRB studies and argues that there likely exist many temporally narrow bursts missed due to instrumental smearing. Giant radio pulses (GRP) from pulsars have typical widths of microseconds but a few at the nanoseconds timescale have been detected (Soglasnov et al. 2004). The computational complexity is enormous for major FRB surveys like those of ASKAP and CHIME/FRB, which search many radio beams and seek both to localize FRBs and detect them at a high rate. As a result, these searches limit their blind detection temporal resolution for detection to ~ 1 ms. In contrast, each unit of GREx receives only one signal stream with modest daily upload of candidates to Caltech. Thus, each GREx unit can undertake sub-millisecond pulses and in due course routinely explore the radio sky at greater resolution. Next, FRBs appear to have strong frequency structure. The usual approach of realizing higher sensitivity

as \sqrt{B} where B is the bandwidth is no longer optimal. However, by undertaking sub-band searches, the ultra-wideband of GReX acts as a very broad frequency field of view.

Galactic Magnetars The mega Jansky burst ST 200428A from SGR 1935+2154 solidified a bridge between the enigmatic extragalactic FRB phenomenon and a known physical object. It also fills in an important chasm in the luminosity function of coherent radio pulses, as it was considerably more energetic than any known Galactic burst, but a couple of orders of magnitude less energetic than the weakest known FRBs. As demonstrated by the multi-telescope, multi-wavelength campaign on SGR 1935+2154, the value of having such a magnetar nearby cannot be overstated. Even the highly-active repeating FRB 180916.J0158+65, at just ~ 150 Mpc, is much too far to reasonably expect a high-energy detection. The recent discovery of the low-DM repeater FRB 20200120E came within ~ 20 kpc of M81 (Bhardwaj et al. 2021). The source was localized to a globular cluster in M81 (Kirsten et al. 2021) at 3.6 Mpc, falling roughly halfway between SGR 1935+2154 and the FRB 180916.J0158+65 in logarithmic distance. Still, it is not yet known if Galactic FRBs are physically identical to extragalactic FRBs, rather than just phenomenologically similar. Therefore, it is essential that we continue to capture Galactic FRBs and dig deeper into their luminosity function with the sensitivity improvements of GReX.

The dynamic spectra of extragalactic FRBs show several distinct features. They are often band-limited, with downward drifting subpulses (Hessels et al. 2019), known as the “sad trombone” effect. While CHIME/FRB’s detection of FRB 200428 had significant time and frequency structure, it is not currently known if the mega bursts emitted by Galactic magnetars have similar dynamic spectra to extragalactic FRBs. The ultra-wideband receivers of GReX allow us to “catch” the narrowband bursts that STARE2 might have missed, but also to study their dynamic spectra over a 3:1 band—five times larger than the band of STARE2—and with almost 100 times better temporal resolution.

If Galactic mega bursts such as ST 200428A are found to be the same physical phenomenon as extragalactic FRBs, we will be able to answer major open questions in the FRB field. For example, is the coherent radio emission produced in the neutron star’s magnetosphere, or is it produced in a relativistic shock well outside of the light cylinder? What is the origin of periodic activity in repeating FRBs? If bright bursts from Galactic magnetars are found to be meaningfully distinct from other FRBs, then that is proof that multiple mechanisms can produce $\sim 10^{30}$ erg Hz $^{-1}$ radio pulses; this would be evidence for the multiple-class interpretation of the FRB population.

Super-giant pulses from Galactic pulsars Young pulsars like the Crab and millisecond pulsars (MSPs) like PSR 1937+214 are known to emit giant radio pulses. Let us define “super-giant pulses” (SGP) as those with fluence higher than 1 MJy μ s. So far, only the Crab pulsar is known to emit SGPs at the GReX observing frequencies. The Crab GRP rate is a power-law function of \mathcal{F} ; from Bera & Chengalur (2019), we expect $N(> \mathcal{F}) = 10^{-2} \text{ hr}^{-1} (\mathcal{F}/10 \text{ MJy } \mu\text{s})^{-1.8}$. Assuming the typical pulse is broad band in frequency and that known sources such as the Crab will be coherently dedispersed, GReX could detect a 1 μ s pulse at a fluence of a few MJy μ s. From the Crab we expect a rate of,

$$\mathcal{R}_{\text{det}}(> \mathcal{F}) \approx 10^2 \text{ yr}^{-1} (X/5)^{1.8}, \quad (1)$$

where X is the sensitivity improvement of GReX over STARE2. Thus GReX should detect some of the brightest super-giant pulses from Crab-like pulsars in our Galaxy, as well as the LMC and SMC. We note that the Crab’s DM varies by $\sim 10^{-2}$ pc cm $^{-3}$ on timescales of roughly 1 year (Kuzmin et al. 2008), leading to a dispersion delay across our band of $\sim 7 \mu$ s and a reduction of S/N during coherent dedispersion. To account for this effect, GReX will use an up-to-date DM for its coherently dedispersed sources, using higher-sensitivity instruments such as DSA-110 to monitor DM variation. It is also salient that some GRP-emitting pulsars exhibit a “kink” in their energy distribution, such that the powerlaw $N(> \mathcal{F}_{\text{th}})$ flattens in the high-energy tail, making ultra-bright bursts more common (Mahajan et al. 2018).

GRPs have been detected from at least ten sources, mostly either young pulsars or MSPs (Kuzmin 2007; Mahajan et al. 2018; Kuiack et al. 2020). Staelin & Reifenstein (1968) discovered the Crab pulsar via its GRPs only days before an independent group at Arecibo found its normal periodic emission in a custom integer FFT developed for pulsar searching. This history was recounted by Lovelace & Tyler (2012). All GRPs were detected *after* the pulsar or its supernova remnant were discovered, sometimes in targeted searches of pulsars with large light-cylinder magnetic field strengths (Knight et al. 2005). Pulsars are typically not discovered blindly via their giant pulses. The Crab is 10^3 years old, and we expect $\mathcal{O}(10)$ such young neutron stars in the Milky Way, given the Galactic core-collapse rate (Rozwadowska et al. 2021) as well as recent High-Altitude Water Cherenkov (HAWC) observations (Albert et al. 2020).

Their normal radio emission may be beamed away from us, but giant pulses are not from near the polar cap and may have different beaming properties (Philippov et al. 2020). The central compact objects of supernova remnants, which do not produce normal radio emission, may generate sudden bursts of SGPs powered by multipolar magnetic fields (De Luca 2017). While they show no sign of strong pulsar wind nebulae and appear to have weak dipolar magnetic fields, their strong multipolar magnetic fields offers a potential energy source for bright bursts (Viganò & Pons 2012). We emphasize that this scenario is speculative as such bursts have not been observed. The central compact objects of supernova remnants (De Luca 2017), which do not produce normal radio emission, may generate sudden bursts of SGPs powered by multipolar magnetic fields. While they do not exhibit strong pulsar wind nebulae, It is likely that some SGPs from unknown pulsars may be detected by the unprecedented blind search of GREx. A pulse of 30 MJy in flux corresponds to $\nu L_\nu = 1.4 \times 10^{38} \text{ erg s}^{-1}$ at a distance of 2 kpc, so the (non-)detection of such pulses will test whether giant pulse isotropic-equivalent luminosity can (temporarily) exceed the spin-down luminosity of the pulsar.

Extragalactic FRBs GREx’s wide, shallow survey strategy also allows us to probe the nearby, ultra-bright extragalactic FRB population. While the primary science function of the instrument is as a Galactic explorer, we might expect $\mathcal{O}(1)$ FRBs from external galaxies over the instrument’s life time. Extrapolating from the ASKAP fly’s eye survey (Shannon et al. 2018), $N(>\mathcal{F}) \simeq 5 \times 10^3 \text{ sky}^{-1} \text{ yr}^{-1} (\mathcal{F}/100 \text{ Jy ms})^{-3/2}$ (see Fig. 3 of Lu & Piro 2019), to the fluence threshold of GREx, one obtains the detection rate

$$N_{\text{det}}(> \mathcal{F}_{\text{th}}) = 0.45 \text{ yr}^{-1} \left(\frac{50 \text{ kJy ms}}{\mathcal{F}_{\text{th}}} \right)^{3/2}. \quad (2)$$

This rate is highly sensitive to the logarithmic slope of the FRB brightness distribution, as we are extrapolating over nearly three orders of magnitude in fluence. If the source counts are flatter than the Euclidean value of -3/2 in the ultrabright tail, GREx might detect multiple extragalactic FRBs. There may also exist a large population of very narrow bursts that ASKAP would have missed due to its relatively coarse time and frequency resolution.

Solar Astronomy GREx will have continuous coverage of the sun with $\sim 10 \mu\text{s}$ sampling and high frequency resolution over a large bandwidth. We will therefore have access to detailed dynamic spectra of fast solar phenomena such as “millisecond spike bursts” (Wang & Xie 1999). We will be able to study Type IV radio bursts, which are likely generated through coherent electron cyclotron maser (ECM) emission (Wang & Xie 1999; Liu et al. 2018).

We remark on two questions at the end of this section. STARE2 could see approximately 25% of the northern sky, meaning at most Earth rotational phases it would not have seen the FRB-like event from SGR 1935+2154. This explains the importance of covering the entire sky for rare but bright events. A world-wide GREx network (as described above) can be built for under a million dollars. Brilliant bursts such as FRB 200428 can be detected via the side-lobes of powerful facilities; indeed, that is how CHIME/FRB discovered FRB 200428. In the northern hemisphere, CHIME/FRB and GREx-I will cover a large portion of the visible sky from 400 MHz to 2 GHz, with 100 MHz of overlap at 750 MHz. This will allow for future symbioses similar to the joint discovery of FRB 200428-like events.

Low frequency facilities such as MWA and LWA naturally enjoy large field-of-view. However, computational costs and interstellar scattering increase as one attempts blind searches at lower frequencies. In the following section we carry out detailed modelling of the magnetars whose bursts we hope to detect.

3. GALACTIC RADIO EXPLORER: IMPLEMENTATION

The basic unit of GREx has a field-of-view of ~ 1.5 steradian and a frequency range of 0.7–2 GHz. We will search data down to $\sim 10 \mu\text{s}$. RFI rejection and crude localization (via timing) requires three units separated by at least one hundred kilometers. We call such a triplet as “cluster”. To cover the entire sky would require eight clusters (four in the North separated by 80 degrees in longitude and four in the South). Thus, a full-up GREx network would have 24 unit systems. Reducing the unit cost is important and is an engineering requirements in the GREx pilot phase. During GREx Phase I we will build a cluster with a 3:1 radio band and, thanks to novel LNAs, sensitivity at least twice that of STARE2. Combined, the increase in sensitivity relative to STARE2 could be as much as a factor of five. We are able to achieve such improvements by piggy-backing on the advances in electronics and antenna design provided by DSA-110 and DSA-2000. Leveraging this work, we will have the lowest system noise temperature (approximately 20 K) yet achieved without cryogenic cooling in the proposed frequency range. While this is our starting point, there is enough flexibility to cater the feed and back-end design to GREx’s science goals, for example trading field of view

Table 1. GReX: Top-level specifications for search

Specification	Value
Band	0.7–2 GHz
Tsys	25 K
Polarization	dual/linear
field-of-view	1.5 steradian
Sampling time	32 μ s (initial) / 8 μ s (hardware)
Channel width (700-1650 MHz)	116 kHz
Channel width (1650-2000 MHz)	42 kHz
Fluence	100 kJy for 1-ms burst
Timing	link to GPS (\pm 10 ns)

for forward gain or shifting the frequency range on a per-site basis to avoid RFI. Similarly, the RFI excision for each cluster of GReX antennas will likely need to be tailored to the local RFI environment, even if the algorithms are common across locations.

We have chosen the GReX configuration over, for example, a focal-plane phased-array without a reflector² for the following reasons: The added complexity and cost related to developing such a system would be non-trivial, as would the increased cost of digitization, channelization, and beamforming compute hardware that follow from having more feeds. The current feed design provides a frequency-independent beamwidth, and a single Stokes I beam requires only two digital backends per antenna, one for each polarization. Therefore, if our goal is to monitor the whole sky continuously with high time and frequency resolution, we find that the most effective way is to deploy simple single radiometer systems around the world. Another suggestion for an all-sky Galactic FRB survey relied on Citizens-Science and cellular communication devices to search for ~ 10 GJy bursts (Maoz & Loeb 2017). However, the detection of ST200428A just above the STARE2 threshold established that the Galactic FRB brightness distribution cannot be very flat and Giga bursts are likely exceedingly rare.

With a world-wide GReX system that includes both more sky coverage and more exposure to the Galactic plane, we anticipate more than an order of magnitude increase in detection rate over STARE2. To achieve this, we aim to create an assembly kit that can be shipped at cost to interested parties around the world.

3.0.1. Wideband Antenna

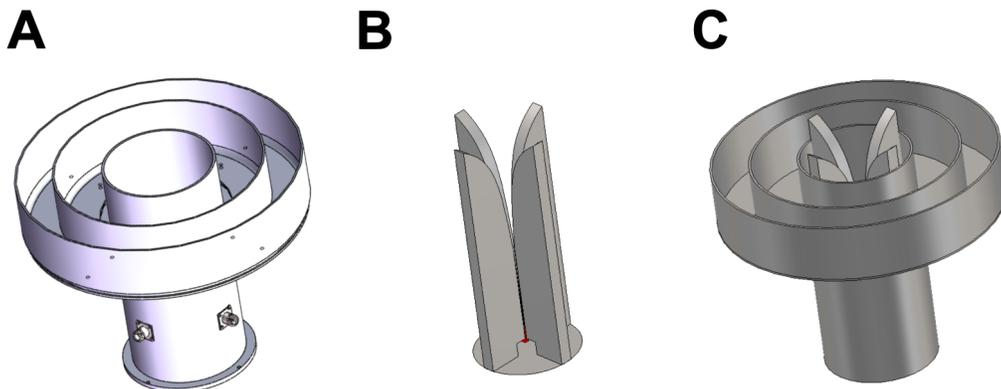


Figure 3. (A) The current STARE2 low-cost “cake-pan” antenna which delivers uniform beam-width and excellent efficiency but over a limited bandwidth. (B) Quad-ridge structure added to the cake-pan delivers wider bandwidth while maintaining a low-cost design. (C) The assembled quad-ridge choke horn structure concept to be used for GReX.

² <https://old.astron.nl/r-d-laboratory/ska/embrace/embrace>

The current “cake-pan” antenna of STARE2 is fabricated from a 6”-diameter aluminum pipe surrounded by two cake pans which reduce spillover and increase efficiency, providing a low-cost solution that delivers uniform beam-width across the 256 MHz band.

Here, we propose to use a quad-ridge horn with a choke-ring structure (Figure 3) for wide-beam performance over a wide frequency range. The design is based on the quad-ridge flared horn (QRFH) technology, developed at Caltech by graduate student Ahmed Akgiray³ and his advisor Dr. Sandy Weinreb. To take advantage of the cost-effective design of the cake-pan antenna, the quad-ridge structure will be integrated with the choke-rings (Figure 3). The choke-ring structure reduces side and back-lobes resulting in a near-symmetric beam pattern. In Figure 4, the beam is exemplified at 1.4 GHz, and the wide, near-constant, full-width-at-half maximum (FWHM) presented over frequency. The quad-ridge structure enable dual linear polarization within a compact footprint, and good impedance match to low-cost 50 Ω coaxial connectors resulting in low input-reflection coefficient over the wide frequency band. To reduce the contribution of noise from ground pick-up to only a few K (Figure 7), a shield underneath the antenna will be used.

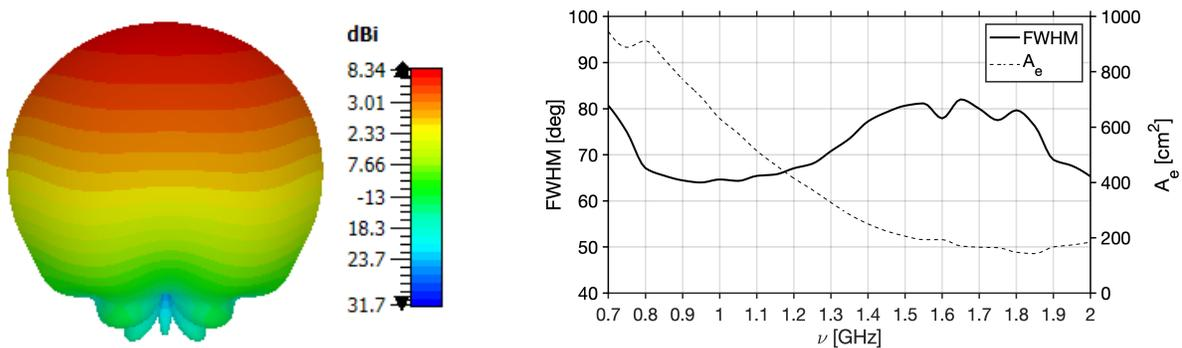


Figure 4. (left): Polar representation of the beam at 1.4 GHz. right): Simulation of beam full-width-at-half maximum (FWHM) in degrees and effective area, A_e , as a function of frequency, ν (in GHz).

3.0.2. Low Noise Amplifiers (LNAs)

A break-through in low noise amplifier (LNA) technology has occurred in the past few years and enables a sensitivity improvement of a factor of 3 compared to the monitors used for the previous STARE2 detection. This can be achieved by reducing the noise temperature of the LNA from 32 K to 10 K and contributions of feed spillover and other losses from 28 K to 10 K to improve the system noise temperature from 60K to 20K. This can be accomplished without the utilization of cryogenic coolers which are costly, require much AC power, and require considerable maintenance.

This LNA break-through has been demonstrated in the DSA110 array at the Caltech Owens Valley Radio Observatory (OVRO) where a system noise of 25 K has been measured on 25 dual-linear polarization 4.6 m paraboloidal reflector antennas operating in the 1.28 to 1.53 GHz frequency range. The LNA for this project is summarized in Figure 5 and fully described in a paper (Weinreb & Shi 2021). The key elements for this low noise are an extremely high performance (Fmax of 550 GHz) high-electron-mobility-transistor (HEMT) on an indium-phosphide (InP) substrate Type pH-100 discrete InP HEMT⁴ and an extremely low loss (<0.05 dB) matching network from the chip transistor pads to the input connector, A brief description of the LNA has been presented at a workshop Weinreb & Shi (2021)⁵.

Our goal for GREX is an LNA for 0.7 to 2 GHz with frequency-averaged noise temperature under 10K. This is challenging due to the required bandwidth of the input matching network to transform 50 ohm impedance of the feed to the optimum impedance driving the transistor which is known from previous studies. This network must have extremely low loss with the realization that 0.1 dB of loss adds 7 K to the noise temperature. There are two approaches to this challenge illustrated in Figure 6: 1) a more complex, but very low loss, input matching network, and 2) cooling just the transistor chip to -40 °C using a Peltier effect solid-state micro-cooler. Using computer-aided-design optimization with high-frequency structure simulator (HFSS) electromagnetic modeling software, a shunt stub

³ Akgiray’s 2013 Caltech PhD is a convenient reference: <https://thesis.library.caltech.edu/7644/>

⁴ Diramics AG, Zurich, <https://diramics.com/products/>

⁵ <https://events.mpifr-bonn.mpg.de/indico/event/154/session/4/contribution/27>

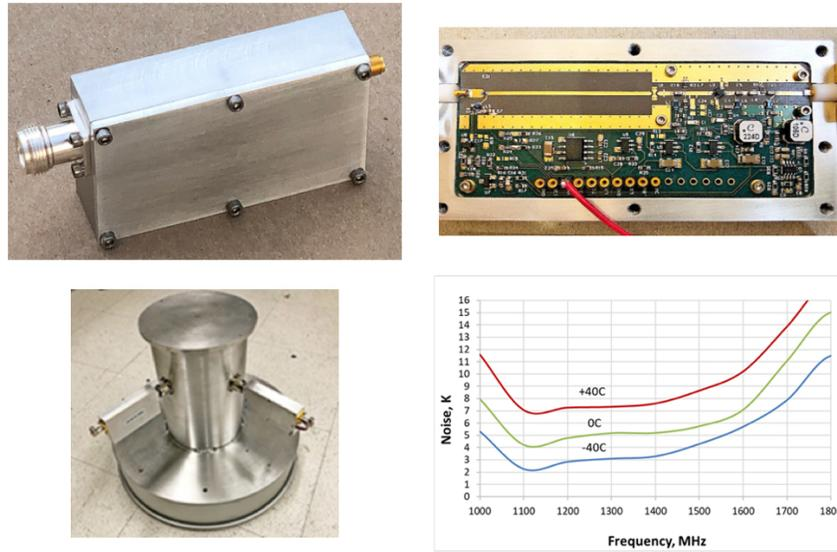


Figure 5. The DSA-110 LNA showing exterior view (top left), interior view (top right), as mounted on the DSA-110 feed (bottom left), and noise temperature vs frequency at 3 temperatures (bottom right). The LNA requires no wires for bias or control; the bias of +5V is supplied on the output coaxial line with control of an internal noise calibration source by a 32kHz tone on this output line.

The input network has been optimized to give a frequency-averaged noise temperature of 10.1K with operation at 25 °C or approximately 5 K less noise by cooling to -40 °C. Analytic models of the loss and capacitance of the Tee connection were not available so a field analysis utilizing finite elements to solve the Maxwell equations was required. A major challenge with cooling to -40 °C is the condensation of water and ice on the transistor. To prevent this over a long period of time, both high vacuum or pressurization with a low thermal conductivity gas such as argon or xenon are being investigated. There is risk to the cooling and our next step will be to construct a prototype LNA with the wideband input network, measure the LNA noise in a laboratory test setup, and then, measure the system noise with the feed including the ground radiation shield.

Following the LNAs additional amplification, filtering, and perhaps frequency conversion will be required to drive the A/D converters and the digital spectrometer. These can be more conventional RF design modules similar to those used in DSA-110 but with wider bandwidth.

3.0.3. Digital back-end

We propose to use SNAP-2 platform⁶ which allows direct sampling (5 Giga-samples per second, or 5 Gsps) of the entire 0.2–2 GHz RF signal to process the 0.7–2 GHz bandwidth. The ADCs sample at 10-bit precision which we believe is sufficient to excise strong RFI that is present in the band of interest to us. We will implement a standard four-tap polyphase filter-bank, using a channelization scheme described below. Following detection in each polarization we will integrate to the desired time resolution, optimally re-quantized to 8-bit precision, and streamed across a 40 GbE direct connection to a computer server (data rate of 8 Gbps). The use of a 40 GbE connection permits streaming voltage data to the server for buffering for the entire usable bandwidth.

As we hope to search the radio sky at $\mathcal{O}(10\ \mu s)$, we must account for intrachannel dispersion smearing. This effect refers to temporal broadening caused by the dispersion delay between adjacent frequency channels and is given by the following equation,

⁶ This includes a Kintex Ultrascale FPGA fed by dual FMC-mounted 5GAD ADCs. Both are supplied by the Institute for Automation in Beijing, China

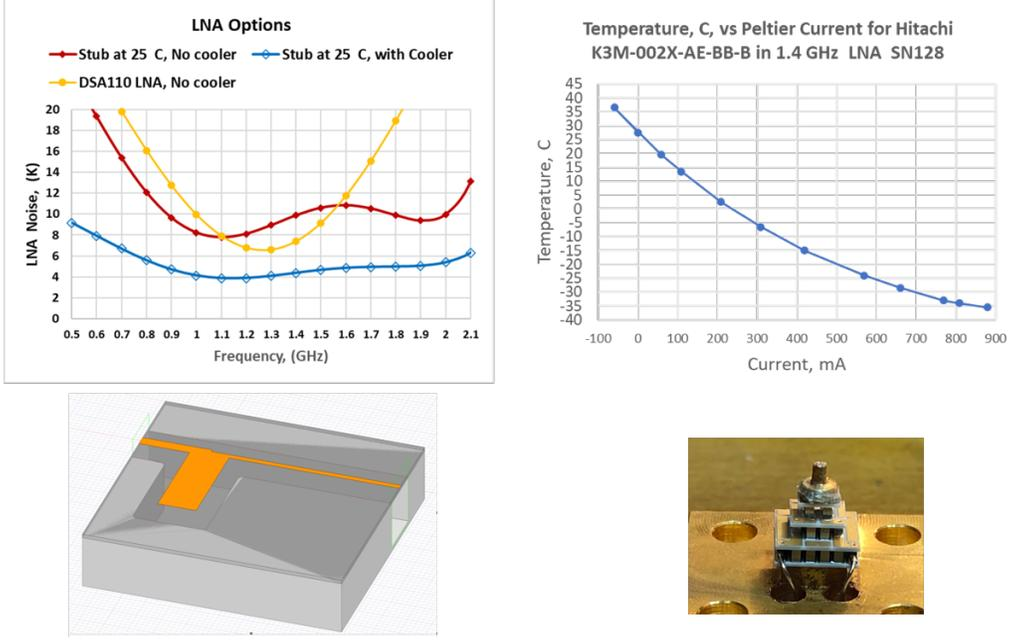


Figure 6. (left) Modeled LNA noise temperature in red without a microcooler, averaging 10.1 K, and with the shunt stub input matching network shown below. (right) Measured physical temperature of a transistor chip mounted on the 6mm high microcooler shown below.

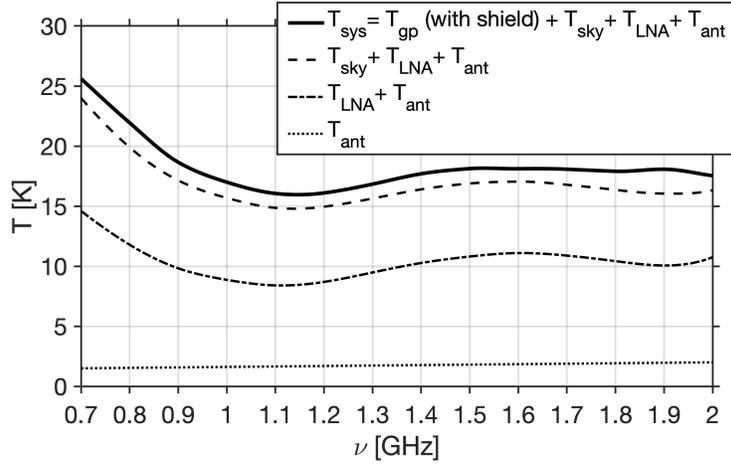


Figure 7. Simulation of system temperature, separated as contributions from ground pick-up (T_{gp}), sky (T_{sky} ; i.e. CMB, Galaxy, atmosphere), the low-noise amplifiers (T_{LNA}), and losses in the wideband antenna (T_{ant}). A ground radiation shield in the form of a square with 4 m sides and 0.3 m, slightly angled, walls reduce the ground pick-up to a few K. A study for optimal shield-material and shape will be done to weight costs (mesh or solid material; curved or flat) and benefit (T_{gp}).

$$t_{\text{DM}} = 8.3 \text{ DM} \left(\frac{\Delta\nu}{1 \text{ MHz}} \right) \left(\frac{\nu_c}{1 \text{ GHz}} \right)^{-3} \mu\text{s}. \quad (3)$$

where ν_c is the observing frequency and $\Delta\nu$ is the frequency resolution. The total smearing is then the quadrature sum of the sampling time and the intrachannel dispersion term,

$$t_{\text{smear}} = \sqrt{t_{\text{samp}}^2 + t_{\text{DM}}^2}. \quad (4)$$

With 16,384 channels across the full band centered on 1.35 GHz, this term is $100 \mu\text{s}$ at the DM of SGR 1935+2154, and we could not achieve our proposed $\mathcal{O}(10 \mu\text{s})$ timescale at such a DM. In order to preserve our high-time resolution

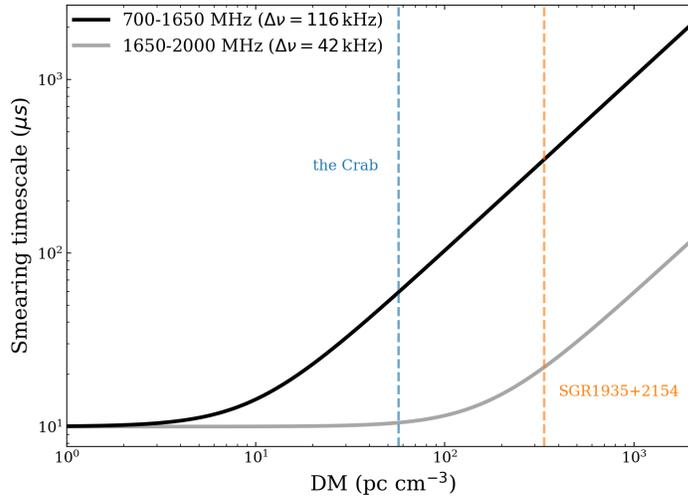


Figure 8. Temporal smearing curves for the two sub-bands of GReX plotted as a function of DM. The top 350 MHz of our band will have finer spectral channels, preserving our ability to search down to tens of microseconds even for high-DM sources.

search for sources in the Galactic plane that may also have high DM, we will implement a hybrid channelization scheme. The top 350 MHz of our band will have 42 kHz resolution (8192 channels) and the bottom 950 MHz will have 116 kHz resolution (8192 channels as well). The single pulse search will combine candidate information between the bands, without loss of information. The smearing curves for both sub-bands are plotted as a function of DM in Fig. 8.

3.0.4. Algorithm & Analysis Computer

GReX’s real-time detection pipeline and computing architecture will be tailored to the instrument’s broad radio band and high time resolution; the traditional `Heimdal1` package, which was used for STARE2, is not well suited to the wide band of GReX, the top of whose frequency range is three times the lower frequency. We will employ a “sub-band” dedispersion algorithm, in which GReX’s large frequency range will be apportioned into uniform chunks in ν^{-2} that will be searched independently and later combined. To this end, we will customize the fast dedispersion algorithm `FDMT` (Zackay & Ofek 2017), which allows for sub-band searching and optimally detecting FRBs with significant frequency structure using the Kalman filter⁷. GReX will thereby serve as a proof-of-concept for future ultra-wideband surveys such as DSA-2000 and the funded Canadian project CHORD (Vanderlinde et al. 2019).

The computer server will be equipped with sufficient processing power to reject impulsive RFI in real time, and to search for FRBs. Data will be piped through the analysis software using the `psrdada` framework. The RFI rejection, dedispersion, and pulse finding will be implemented on an Nvidia Quadro RTX4000 GPU. The hardware is well suited to a final-stage machine learning classifier which will send out reliable, real-time triggers to other facilities Connor & van Leeuwen (2018). RFI excision will be done using a common set of modular algorithms. Since we expect each GReX site to have different RFI characteristics, the exact parameters of those algorithms will be tailored to the site. While the final set of sites is not yet known with certainty, we plan to choose locations whose RFI environment is relatively clean.

We plan to reserve roughly a dozen DM channels to be coherently dedispersed when known pulsars are in the beam, enabling us to search for super-giant radio pulses without the deleterious effects of instrumental smearing. The DMs will correspond to known millisecond pulsars and young pulsars, the sources most likely to emit giant pulses.

Our design allows for upgrades to be explored by the group, in response to the evolving scientific landscape. For example, we can modify the digital firmware to stream voltage data for buffering on the server, such that when a pulse is detected the data can be analyzed with better time and frequency resolution. Additionally, we have sufficient processing power on the FPGA to derive full-polarization data, if needed.

⁷ https://bitbucket.org/bzackay/kalman_detector/src/master/

3.1. Future Stations

One of the goals of GReX is to expand University-based radio observatories in the United States. Specifically, we envisage a future effort to place unit systems at sites that are managed or accessible to Universities, with emphasis on state universities in the US with the intention of accelerating radio astronomy education for undergraduates. We also feel that a GReX cluster in Canada, for example at the Algonquin Radio Observatory (ARO) would help with both sky coverage and would allow for continuous coverage at 400–2000 MHz in the Northern Hemisphere. RFI studies will be undertaken of potential future site. GReX will serve this purpose explicitly as a test antenna at the proposed DSA-2000 site, Big Smoky Valley, Nevada, where it will both act as an RFI monitor and carry out its primary science. For clusters within \sim thousands of km of one another, we will offset the antennas in pointing to minimize overlap on sky.

During GReX Phase II we plan expand beyond the United States, starting with Australia and India in order to build up 24/7 coverage of the Galactic plane, where the majority of magnetars reside. Clusters of antennas in both Western Australia and Tasmania would provide 120 deg of coverage in right ascension, if they each point 7.5 deg off-zenith. A set of three antennas in India could be located at GMRT. We also hope to deploy GReX instrumentation in Western Europe, the Middle East, and elsewhere until we have an international network spanning the full sky's 4π steradians. We anticipate that this will require roughly 25 hardware kits.

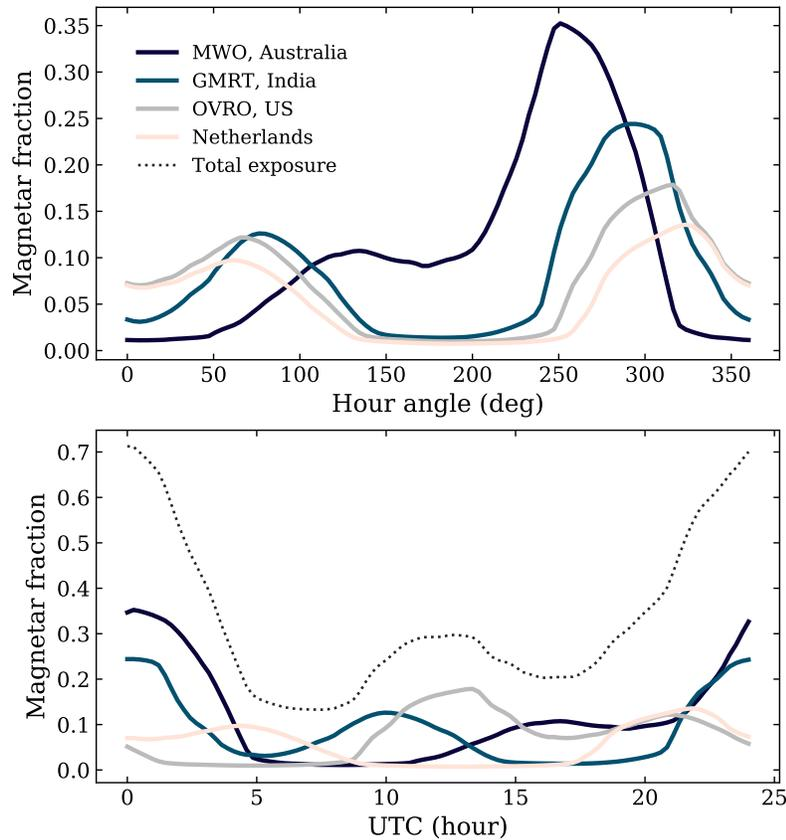


Figure 9. Modelling of the fraction of Galactic magnetars that are within the FoV of a GReX antenna for different potential cluster locations around the world. The top panel shows this fraction as a function of hour angle (HA). The bottom panel shows the same fraction vs. UTC, accounting for the different RAs to which each location is exposed at a given time. The dotted line is the combined visible fraction of Galactic magnetars for the whole GReX-II array.

4. MODELLING

By sending GReX clusters to southern latitudes we will gain exposure to the bulk of the Galactic plane, where magnetars reside. We also aim to increase our coverage in right ascension by deploying clusters at a range of longitudes. Using molecular gas and star formation as a proxy for the magnetar distribution in the Milky Way, we model the fraction of Galactic magnetars to which GReX will be exposed at a given time. Combining this with the increased sensitivity of each unit, we can forecast the expected Galactic FRB rate and speculate on the GRPs we can find from pulsars.

We take the Planck HFI 857 GHz map and assume we have clusters in the Southwestern United States, India, Western Europe and Australia. Based on Figure 4, we take the GReX antenna’s FWHM to be 80 deg. We compute to total visible material in the Planck 857 GHz map at a given time to estimate the fraction of Galactic magnetars that are observable at each cluster. The top panel of Figure 9 shows this fraction as a function of hour angle at four locations. Clearly, the heightened exposure to the inner Galactic plane gives the southern stations an advantage. The bottom panel show the same fraction, but as a function of coordinated universal time (UTC), including the instantaneous total exposure of all stations combined. For more than half of the time, this configuration is exposed to more than 30% of the magnetars in our Galaxy. Eventually the network will see the whole sky all of the time.

4.1. Event rates

The system temperature of GReX is expected to be ~ 2.6 times lower than that of STARE2, thanks to the aforementioned improvements in front-end electronics. Its antennas will have five times as large a frequency band, and the addition of southern clusters will give GReX more instantaneous sky coverage and increased exposure to the Galactic plane. Extrapolating from the STARE2 detection of one burst in 448 days on sky, we can estimate the detection rate of GReX-I and GReX-II. The detection rate is given by the product of the survey’s field of view, Ω , and the source

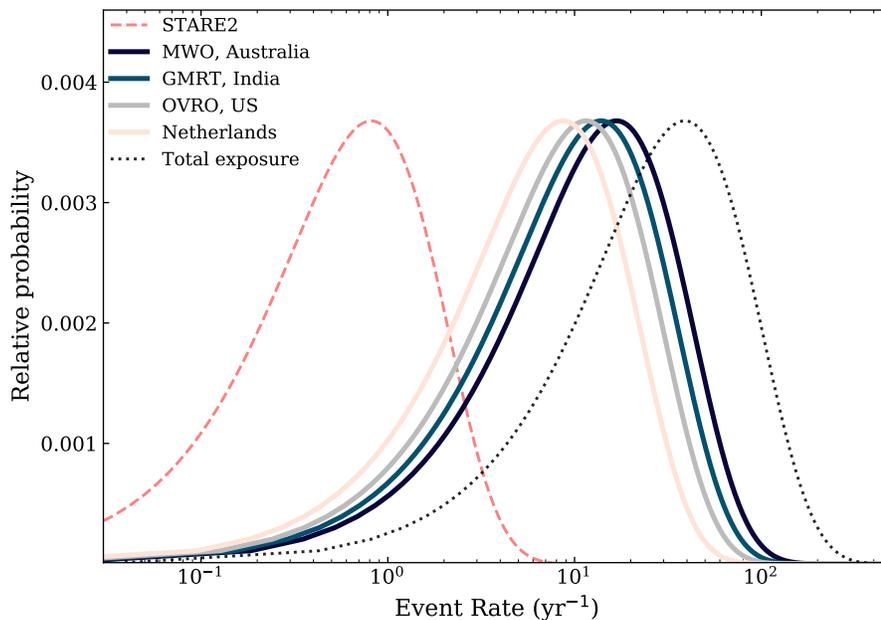


Figure 10. The event rate distributions based on one FRB-like event detected by STARE2 in 448 days on sky. The relative probabilities vs. detection rate are plotted for individual GReX clusters around the world (solid) as well as a hypothetical GReX-II array (dotted) that has antennas in Australia, the Netherlands, India, and the United States. Even if FRB 200428 were a rare event and STARE2 and CHIME/FRB were “lucky” to have detected it, the full array will likely find multiple such events per year.

density on sky above the instrument’s detection threshold, $N(> s_{\min})$. We take the source brightness distribution to

be a power-law such that, $N(> s_{\min}) \propto s_{\min}^{-\alpha}$, where s_{\min} is given by the radiometer equation. Assuming a baseline rate for STARE2, \mathcal{R}_{S2} , the detection rate of GREX-II will be a sum over all antenna clusters around the world, weighted by their average exposure to the Galaxy’s magnetars compared to STARE2. We call this weight for the i^{th} GREX cluster location, w_i . This gives,

$$\mathcal{R}_{\text{GREX}} = \mathcal{R}_{S2} \sum_i^{n_{\text{clust}}} w_i \frac{\Omega_i}{\Omega_{S2}} \left(\frac{\text{SEFD}_{S2}}{\text{SEFD}_i} \sqrt{\frac{B_i}{B_{S2}}} \right)^\alpha, \quad (5)$$

where SEFD refers to the system-equivalent flux density, or the ratio of system temperature to gain, T_{sys}/G . Assuming each GREX unit has the same FoV as STARE2 and that the pointings are mostly independent, we get

$$\mathcal{R}_{\text{GREX}} = 1/448 \text{ days}^{-1} \left(2.6\sqrt{5} \right)^\alpha \sum_i w_i. \quad (6)$$

We note that the $\sqrt{5}$ factor implicitly assumes that the burst spectrum is both flat and broadband, which may be optimistic. Still, we do not have a good model for the spectral structure of FRBs in general, and ST 200428A/FRB 200428 was brighter at 1.4 GHz than at 0.6 GHz, so for the sake of simplicity we have assumed equal power across the GREX band. Equation 5 computes the maximum-likelihood value of the event rate based on STARE2’s sole detection, but we must include the uncertainty associated with just one burst. Using Bayes’ theorem we know,

$$P(\mathcal{R}|N) = \frac{P(N|\mathcal{R})P(\mathcal{R})}{P(N)}, \quad (7)$$

where in this case $N = 1$. Taking a flat prior on \mathcal{R} and assuming the detection of new bursts follow Poissonian statistics, we can invert Equation 7 to get,

$$P(N=1|\mathcal{R}) = \mathcal{R} e^{-\mathcal{R}}. \quad (8)$$

By scaling \mathcal{R} for GREX using Equation 5, we can calculate the probability distribution in detection rate after the improved sensitivity and exposure to Galactic magnetars. This is shown in Figure 10.

The forecasting we have presented has extrapolated from STARE2’s single detection of ST 200428A/FRB 200428 using the modelled distribution of magnetars in the Milky Way. The result is a Poissonian confidence interval for GREX, but this range is *not* the rate of unique GREX detections. A burst in the Northern Hemisphere could also be detected by CHIME/FRB, barring observing frequency differences. Furthermore, an X-ray all-sky monitor might observe high energy activity from a Galactic magnetar, allowing other radio instruments to spend time on that source during its active phase and detect a radio burst that GREX would also see. While this detracts from our unique discovery capability, it is likely that multiple detections of the same event will add scientifically to the discovery. Together, CHIME/FRB and GREX will span the full range between 400 and 2000 MHz, overlapping only between 700–800 MHz.

5. SUMMARY

We have proposed GREX, a radio all-sky monitor that will detect the brightest bursts in the Galactic sky on sub-millisecond timescales. GREX Phase II will be an international network of ultra-wideband, high performance antennas that will continuously search for Galactic FRBs and super giant pulses from radio pulsars. Each hardware component will be low-cost and replicable, such that clusters of at least three GREX antennas can be shipped as an assembly kit around the world to span a wide range of latitude and longitude. The software and firmware back-end will also be standardized such that each system will require little intervention once running. We expect to find multiple new FRB-like events from Galactic magnetars each year. As the first wide-field, blind single-pulse survey at the microsecond level, we should find new super giant pulses from Galactic pulsars, as well as previously-unknown phenomena.

ACKNOWLEDGEMENTS

We thank Dale Gary and Dan Werthimer for helpful discussions, as well as an anonymous referee for valuable advice on the manuscript.

REFERENCES

- Albert, A., Alfaro, R., Alvarez, C., et al. 2020, ApJ, 905, 76, doi: [10.3847/1538-4357/abc2d8](https://doi.org/10.3847/1538-4357/abc2d8)
- Bera, A., & Chengalur, J. N. 2019, MNRAS, 490, L12, doi: [10.1093/mnrasl/slz140](https://doi.org/10.1093/mnrasl/slz140)

- Bhardwaj, M., Gaensler, B. M., Kaspi, V. M., et al. 2021, arXiv e-prints, arXiv:2103.01295.
<https://arxiv.org/abs/2103.01295>
- Bochenek, C. D., McKenna, D. L., Belov, K. V., et al. 2020a, *PASP*, 132, 034202, doi: [10.1088/1538-3873/ab63b3](https://doi.org/10.1088/1538-3873/ab63b3)
- Bochenek, C. D., Ravi, V., Belov, K. V., et al. 2020b, *Nature*, 587, 59, doi: [10.1038/s41586-020-2872-x](https://doi.org/10.1038/s41586-020-2872-x)
- CHIME/FRB Collaboration, Andersen, B. C., Bandura, K., et al. 2019, *ApJL*, 885, L24, doi: [10.3847/2041-8213/ab4a80](https://doi.org/10.3847/2041-8213/ab4a80)
- Chime/Frb Collaboration, Amiri, M., Andersen, B. C., et al. 2020, *Nature*, 582, 351, doi: [10.1038/s41586-020-2398-2](https://doi.org/10.1038/s41586-020-2398-2)
- Connor, L. 2019, *MNRAS*, 487, 5753, doi: [10.1093/mnras/stz1666](https://doi.org/10.1093/mnras/stz1666)
- Connor, L., Miller, M. C., & Gardenier, D. W. 2020, *MNRAS*, 497, 3076, doi: [10.1093/mnras/staa2074](https://doi.org/10.1093/mnras/staa2074)
- Connor, L., & van Leeuwen, J. 2018, *AJ*, 156, 256, doi: [10.3847/1538-3881/aae649](https://doi.org/10.3847/1538-3881/aae649)
- Cordes, J. M., & Chatterjee, S. 2019, *ARA&A*, 57, 417, doi: [10.1146/annurev-astro-091918-104501](https://doi.org/10.1146/annurev-astro-091918-104501)
- De Luca, A. 2017, in *Journal of Physics Conference Series*, Vol. 932, *Journal of Physics Conference Series*, 012006, doi: [10.1088/1742-6596/932/1/012006](https://doi.org/10.1088/1742-6596/932/1/012006)
- Fonseca, E., Andersen, B. C., Bhardwaj, M., et al. 2020, *ApJL*, 891, L6, doi: [10.3847/2041-8213/ab7208](https://doi.org/10.3847/2041-8213/ab7208)
- Gajjar, V., Siemion, A. P. V., Price, D. C., et al. 2018, *ApJ*, 863, 2, doi: [10.3847/1538-4357/aad005](https://doi.org/10.3847/1538-4357/aad005)
- Hessels, J. W. T., Spitler, L. G., Seymour, A. D., et al. 2019, *ApJL*, 876, L23, doi: [10.3847/2041-8213/ab13ae](https://doi.org/10.3847/2041-8213/ab13ae)
- Kirsten, F., Snelders, M., Jenkins, M., et al. 2020, arXiv e-prints, arXiv:2007.05101.
<https://arxiv.org/abs/2007.05101>
- Kirsten, F., Marcote, B., Nimmo, K., et al. 2021, arXiv e-prints, arXiv:2105.11445.
<https://arxiv.org/abs/2105.11445>
- Knight, H. S., Bailes, M., Manchester, R. N., & Ord, S. M. 2005, *ApJ*, 625, 951, doi: [10.1086/429533](https://doi.org/10.1086/429533)
- Kuiack, M., Wijers, R. A. M. J., Rowlinson, A., et al. 2020, *MNRAS*, 497, 846, doi: [10.1093/mnras/staa1996](https://doi.org/10.1093/mnras/staa1996)
- Kuzmin, A., Losovsky, B. Y., Jordan, C. A., & Smith, F. G. 2008, *A&A*, 483, 13, doi: [10.1051/0004-6361:20079211](https://doi.org/10.1051/0004-6361:20079211)
- Kuzmin, A. D. 2007, *Ap&SS*, 308, 563, doi: [10.1007/s10509-007-9347-5](https://doi.org/10.1007/s10509-007-9347-5)
- Liu, H., Chen, Y., Cho, K., et al. 2018, *SoPh*, 293, 58, doi: [10.1007/s11207-018-1280-y](https://doi.org/10.1007/s11207-018-1280-y)
- Lovelace, R. V. E., & Tyler, G. L. 2012, *The Observatory*, 132, 186
- Lu, W., & Piro, A. L. 2019, *ApJ*, 883, 40, doi: [10.3847/1538-4357/ab3796](https://doi.org/10.3847/1538-4357/ab3796)
- Mahajan, N., van Kerkwijk, M. H., Main, R., & Pen, U.-L. 2018, *ApJL*, 867, L2, doi: [10.3847/2041-8213/aae713](https://doi.org/10.3847/2041-8213/aae713)
- Maoz, D., & Loeb, A. 2017, *MNRAS*, 467, 3920, doi: [10.1093/mnras/stx400](https://doi.org/10.1093/mnras/stx400)
- Pastor-Marazuela, I., Connor, L., van Leeuwen, J., et al. 2020, arXiv e-prints, arXiv:2012.08348.
<https://arxiv.org/abs/2012.08348>
- Petroff, E., Hessels, J. W. T., & Lorimer, D. R. 2019, *A&A Rv*, 27, 4, doi: [10.1007/s00159-019-0116-6](https://doi.org/10.1007/s00159-019-0116-6)
- Philippov, A., Timokhin, A., & Spitkovsky, A. 2020, *PhRvL*, 124, 245101, doi: [10.1103/PhysRevLett.124.245101](https://doi.org/10.1103/PhysRevLett.124.245101)
- Pleunis, Z., & Chime/Frb Collaboration. 2021, in *American Astronomical Society Meeting Abstracts*, Vol. 53, *American Astronomical Society Meeting Abstracts*, 236.03
- Pleunis, Z., Michilli, D., Bassa, C. G., et al. 2020, arXiv e-prints, arXiv:2012.08372.
<https://arxiv.org/abs/2012.08372>
- Rajwade, K. M., Mickaliger, M. B., Stappers, B. W., et al. 2020, *MNRAS*, 495, 3551, doi: [10.1093/mnras/staa1237](https://doi.org/10.1093/mnras/staa1237)
- Rozwadowska, K., Vissani, F., & Cappellaro, E. 2021, *NewA*, 83, 101498, doi: [10.1016/j.newast.2020.101498](https://doi.org/10.1016/j.newast.2020.101498)
- Scholz, P., & Chime/Frb Collaboration. 2020, *The Astronomer's Telegram*, 13681, 1
- Shannon, R. M., Macquart, J. P., Bannister, K. W., et al. 2018, *Nature*, 562, 386, doi: [10.1038/s41586-018-0588-y](https://doi.org/10.1038/s41586-018-0588-y)
- Soglasnov, V. A., Popov, M. V., Bartel, N., et al. 2004, *ApJ*, 616, 439, doi: [10.1086/424908](https://doi.org/10.1086/424908)
- Staelin, D. H., & Reifenstein, E. C. 1968, *Science*, 1481, 3
- The CHIME/FRB Collaboration, :, Andersen, B. C., et al. 2020, arXiv e-prints, arXiv:2005.10324.
<https://arxiv.org/abs/2005.10324>
- Vanderlinde, K., Liu, A., Gaensler, B., et al. 2019, in *Canadian Long Range Plan for Astronomy and Astrophysics White Papers*, Vol. 2020, 28, doi: [10.5281/zenodo.3765414](https://doi.org/10.5281/zenodo.3765414)
- Viganò, D., & Pons, J. A. 2012, *MNRAS*, 425, 2487, doi: [10.1111/j.1365-2966.2012.21679.x](https://doi.org/10.1111/j.1365-2966.2012.21679.x)
- Wang, M., & Xie, R. X. 1999, *SoPh*, 185, 351, doi: [10.1023/A:1005101001388](https://doi.org/10.1023/A:1005101001388)
- Weinreb, S., & Shi, J. 2021, *IEEE Trans, on Microwave Th. And Tech.*, 132
- Zackay, B., & Ofek, E. O. 2017, *ApJ*, 835, 11, doi: [10.3847/1538-4357/835/1/11](https://doi.org/10.3847/1538-4357/835/1/11)
- Zhang, C. F., Jiang, J. C., Men, Y. P., et al. 2020, *The Astronomer's Telegram*, 13699, 1

Zhu, W., Wang, B., Zhou, D., et al. 2020, The
Astronomer's Telegram, 14084, 1